

Nb₃Sn MULTICELL CAVITY COATING AT JLAB*

U. Pudasaini², G. Ereemeev^{1,†}, G. Ciovati^{1,4}, M. J. Kelley^{1,2,3},
I. Parajuli⁴, C. E. Reece¹, Md. N. Sayeed⁴

¹Thomas Jefferson National Accelerator Facility, Newport News, VA 23606, U.S.A.

²College of William and Mary, Williamsburg, VA 23185, U.S.A.

³Virginia Tech, Blacksburg, VA 24061, U.S.A.

⁴Old Dominion University, Norfolk, VA 23504, U.S.A.

Abstract

Following encouraging results with Nb₃Sn-coated single-cell cavities, the existing coating system was upgraded to allow for Nb₃Sn coating of CEBAF accelerator cavities. The upgrade was designed to allow Nb₃Sn coating of original CEBAF 5-cell cavities with the vapor diffusion technique. Several CEBAF cavities were coated in the upgraded system to investigate vapor diffusion coatings on extended structures. Witness samples coated along with the cavities were characterized with material science techniques, while coated cavities were measured at 4 and 2 K. The progress, lessons learned, and the pathforward are discussed.

INTRODUCTION

Superconducting radio frequency (SRF) cavities are an integral part of many accelerators. The cavities are typically made of niobium sheets, which are deep-drawn, welded, and post-processed to achieve desirable SRF properties. Besides niobium, several other superconductors may deliver advantages of SRF to accelerators. Among them is Nb₃Sn, a superconducting material that may improve upon SRF properties of niobium thanks to its higher critical temperature and superheating field. Presently, several groups around the world pursue Nb₃Sn development for SRF applications [1–5].

A promising technique called vapor diffusion [6] has been used to deposit μm -thick Nb₃Sn layers onto SRF cavities since 70's [7–10]. At Jefferson Lab, the development originally started with a setup of coating facility for single-cell R&D cavities [11]. The system was designed to coat single-cell R&D cavities using vapor diffusion technique. Early results indicated transition temperatures of about 18 K. Quality factors were measured at about $1 \cdot 10^{10}$ at 4K. The gradient reach in the best cavities was found to be limited by a reproducible Q-slope similar to the one observed at Wuppertal [12, 13]. The Q-slope has been speculated to be fundamental to the Nb₃Sn films, but the more recent results from Cornell group ruled it out [14]. Although Cornell group was replicating the coating approached used at Wuppertal, several cavities coated at Cornell reached magnetic fields above 40 mT without Q-slope [15]. Microscopic examination of coated films has not decisively indicated the reason behind

Q-slope, although surface features/Sn-deficient regions [16] and coating contamination [13] has been put forth. The films are commonly found to comprise columnar Nb₃Sn grains that are roughly the same size as thickness and have no correlation to the underlying Nb grains [17]. Surface features have been also often observed.

Along with single-cell cavity coatings, several multi-cell cavities were coated [13, 18]. Initially, two 2-cell cavities were coated, and later, a modified CEBAF 5-cell cavity was coated. The results again indicated promising transition temperatures and quality factors similar to single-cell results. These efforts prompted us to consider the coating of a CEBAF 5-cell cavities. Further research is required to enable the gradients of interest to CEBAF, which are about 20 MV/m. However, single cell results indicated that accelerating gradient of about 10 MV/m are within the reach, and JLab upgraded injector test facility (UITF), which is currently under construction, is set up to use one quarter cryomodule delivering 10 MV gain to electron beam. Providing 10 MV/m Nb₃Sn-coated CEBAF cavities for such cryomodule will reduce cryogenic needs to operate UITF and will provide a good test bench to test Nb₃Sn cavities in the accelerator environment, which is important, because, except for what appears to have been a short test [19], Nb₃Sn cavities have never been used to accelerate beams. With these goals in mind, an upgrade to the coating system was put forth to enable the coating of the complete CEBAF 5-cell cavities. Fortuitously, the R&D coating system was built with a large enough furnace to allow for a subsequent expansion that can fit CEBAF 5-cell cavities. Herein we present some of the design choices, lessons learned, and the results from first coatings.

CAVITY DEPOSITION SYSTEM

The deposition system comprises two main parts: the furnace that provides a clean heating environment to the coating chamber and the coating chamber that contains the process vapors. The deposition system was originally built for single-cell cavities [11]. In order to coat CEBAF cavities, both the furnace and the coating chamber needed to be upgraded. A new coating chamber was built out of 4 mm niobium sheets into a 17 inch OD by 40 inch long cylinder via rolling half cylinders and electron beam welding them. The chamber was closed from one end with a 4 mm niobium blank, which was deep-drawn into dome shape and electron beam welded to the cylinder shell. The other end of the

* Co-Authored by Jefferson Science Associates, LLC under U.S. DOE Contract No. DE-AC05-06OR23177. This material is based upon work supported by the U.S. Department of Energy, Office of Science, Office of Nuclear Physics.

† grigory@jlab.org

cylinder shell was welded to a 21 inch OD titanium grade 5 flange, which had half-dovetail 0.25" o-ring grooves on both sides. It should be noted that the first choice was a stainless steel flange, because we were looking to avoid having any titanium in the chamber for the reasons discussed in the next section. However, the first attempts to braze a stainless steel flange to the niobium cylinder proved unsuccessful. It was unexpected, because prior experience of brazing 14" OD SS steel flange to niobium cylinder did not have any issues [11]. After a couple of unsuccessful attempts with brazing, the niobium cylinder was TIG welded to a titanium flange. On one side the flange provided vacuum insulation via o-ring to the new furnace door, on the other side o-ring was sealed against zero-length water-cooled reducer. This zero-length reducer allowed to re-use instrumentation and pumping on the existing multiport spool piece and top plate, Fig. 1. In order to accommodate longer cavities the furnace volume had to be increased, which was accomplished by replacing the original flat furnace door with a dome-shaped door and new heat shields. The door itself was procured from Kurt J. Lesker Company according to the specifications provided by Jefferson Lab. The heat shields were built in-house out of 0.015" molybdenum sheets. Six heat shield layers were used similar to the construction in the existing furnace. On the outside the heat shields were supported by a stainless steel support cylinder.

Three niobium rods were attached at the top to the multiport plate and extended downwards into the hot zone. Niobium rods support a 4 mm niobium plate, to which the top flange of a cavity is attached with molybdenum hardware. Niobium blanks were used to cover ports of the CEBAF 5-cell cavities attached using molybdenum hardware. Several type C thermocouples extending into the hot zone were added to monitor the temperature of cavities during coating. The first runs with the thermocouples indicated that a temperature gradient of about 60-80 K exists from bottom to the top of the hot zone, while the three furnace thermocouples outside the coating chamber indicate uniform temperature within 0.3 K. By adjusting the three independently-controlled heating elements of the furnace, the gradient could be reduced to about 20 K. The temperature gradient during cavity coatings depended on the position and geometry of the coated structures.

SINGLE CELL Nb₃Sn COATING

As mentioned in the previous section, the upgrade to the coating system was done with an attempt to avoid titanium contamination. Looking at the RF results from the cavities coated at Wuppertal, Cornell, and JLab, the absence of the Q-slope in Cornell-coated cavities is clear [14]. While there are clear differences in the coating systems between Cornell and JLab, Cornell coating system resembles Wuppertal coating arrangement. Cornell group also follows a coating procedure similar to Wuppertal's [20,21]. One feature, which was noticed to be potentially common to coatings at Wuppertal and JLab, and to be different at Cornell, was the presence

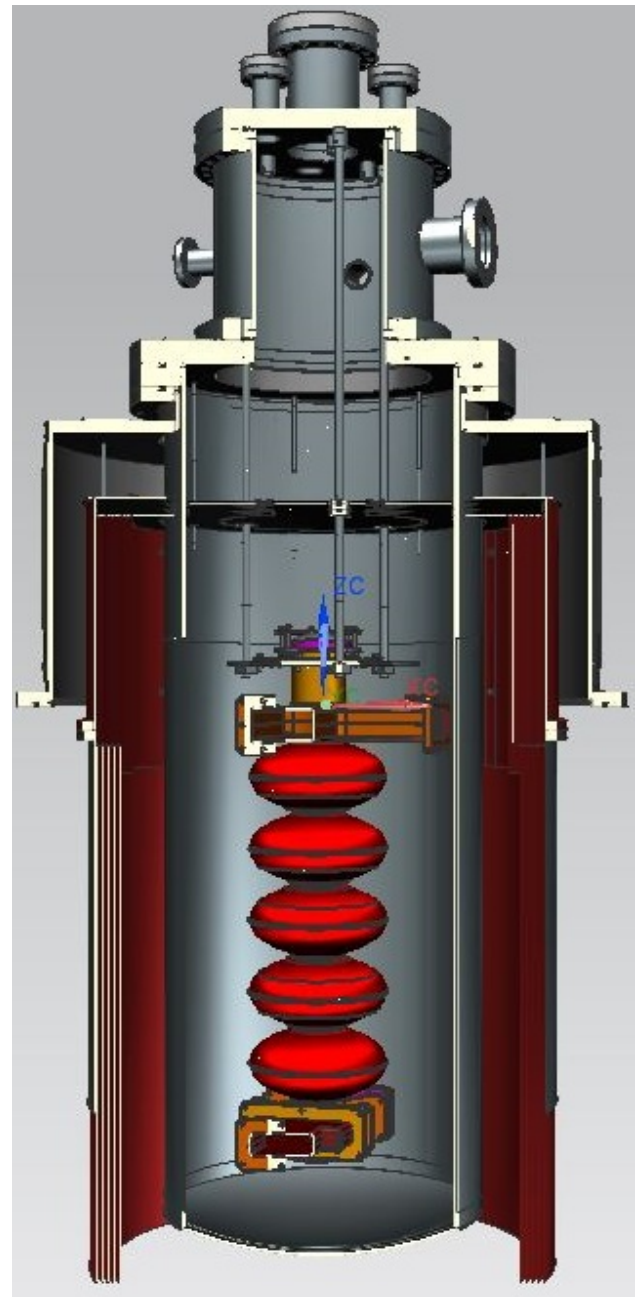


Figure 1: A sketch of the upgraded coating chamber. The outer vacuum vessel of the original furnace, on which this assembly rests, is omitted from the sketch. A CEBAF 5-cell cavities is shown suspended inside the hot zone.

of titanium. SIMS studies of the samples coated at JLab and Cornell showed the higher presence of titanium in JLab samples [4,22]. In the case of the samples coated at JLab, titanium is likely originated from the TIG welds, which were used on the flanges of the sample coating chamber before its construction. In the case of cavities, we speculated that titanium was coming from NbTi flanges on the cavities. Surface studies showed that titanium diffuses into niobium to the depth of about 1 μm at 1200 °C for 3 hours [23]. In

case of Wuppertal coatings, the flanges of at least one of the cavities, which we have, were checked and found to be made out of niobium. However, Peiniger in his description of the coating chamber points out that Ti foils were used on the outside during the coating to maintain RRR of niobium [24]. He also points out that low titanium contamination in the grown Nb_3Sn can be practically hardly avoided, but explains that it was not seen as critical, because even 5 at. % of titanium reduces the critical temperature by only 0.2 K. Since titanium contamination has been shown to affect medium field Q-slope of niobium cavities [23, 25], we speculated that titanium may contribute to the "Wuppertal" slope and took measures to avoid titanium contamination in the new chamber.

Besides the furnace construction and coating arrangement, a single cell 1.3 GHz cavity RDT2, which had NbTi flanges, was re-worked into an all-niobium cavity. Although the cavity reached up to $E_{acc} = 28$ MV/m in the initial baseline testing, the cavity proved to be challenging to reach high gradients after the re-work. The performance issues were linked to the defects found on the equator, and several attempts to coat and baseline the cavity were made. In the latest baseline test the cavity had low-field quality factor of about $2 \cdot 10^{10}$ and quench at $E_{acc} \cong 17$ MV/m at 2.0 K. After the latest baseline test, the cavity was prepared and coated along with another all-niobium cavity SC-IB, which was a large-grain cavity. The cavities shared the reaction space, with RDT2 positioned at the bottom, where Sn and SnCl₂ sources were, and SC-IB at the top mounted to the support plate. Six grams of tin and three grams of SnCl₂ were used for this coating. The temperature profile was the same profile that has been used for all cavity coatings so far [13], but the individual temperatures of the three hot zones were adjusted based on the prior coating experience. After the coating the cavity surface of both cavities visually appeared to be uniformly coated. In Fig. 2 pictures of the top and bottom half cells are shown in the top row and the inspection images with KEK camera [26], which showed that defects are still present in the equator region of RDT2, in the bottom row. After the coating the cavities followed the standard preparation procedure for SRF testing. During RF testing RDT2 developed a small cold leak, but the measurement of the quality factor as a function of field was still carried out. In Fig. 3 the RF measurement of RDT2 is shown at 4 K and 2 K. At 4K the low-field quality factor was about $1.8 \cdot 10^{10}$, and the cavity exhibited a Q-slope. At $E_{acc} = 7$ MV/m the quality factor started to degrade rapidly due to apparently some heating. Some X-rays were observed at $E_{acc} \cong 7$ MV/m. At 2 K the low-field quality factor was about $4.3 \cdot 10^{10}$, and the cavity again exhibited a Q-slope. The cavity was limited to $E_{acc} \cong 10.5$ MV/m by a quench. Following one quench the low-field quality factor degraded to about $1.4 \cdot 10^9$. X-rays were observed above $E_{acc} = 7$ MV/m. In Fig. 4 the RF measurements of SC-IB are shown at 4 K and 2 K. At 4 K the low-field quality factor was about $6.7 \cdot 10^9$. The cavity reached $E_{acc} \cong 10$ MV/m with the quality factor degrading to about $5.3 \cdot 10^9$. At the highest gradient

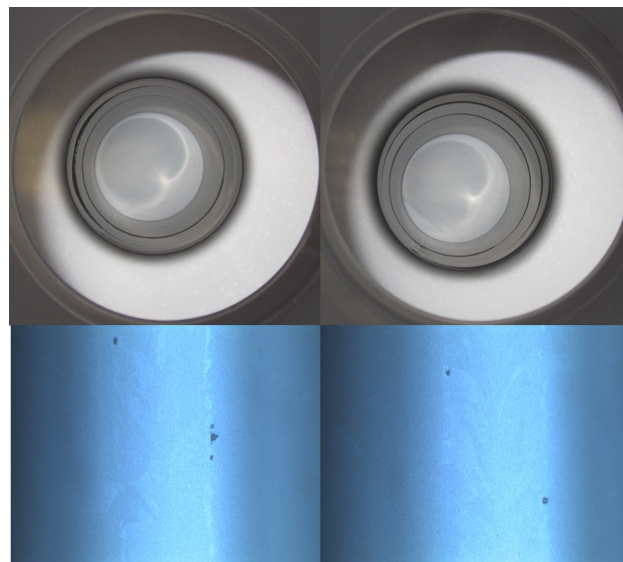


Figure 2: RDT2 pictures from optical inspections. Top row shows camera images of the bottom [left] and the top [right] half cells after coating. The bottom row shows two images of the equator region, where pre-existing defects were observed.

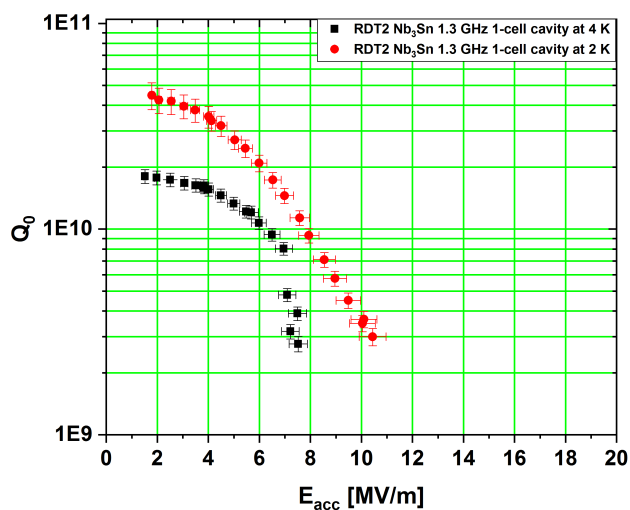


Figure 3: RDT2 test results at 4K and 2K. Low-field quality factors are similar to commonly observed in Nb₃Sn-coated cavities, but note the rapid Q-degradation.

some heating limited the gradient reach. At 2K the low-field quality factor was about $9.5 \cdot 10^9$. The cavity reached $E_{acc} = 14.7$ MV/m with quality factor degrading to about $5.2 \cdot 10^9$. The cavity was limited by a quench. Stainless steel blanks on the cavity ports were estimated to contribute about 4.4 nΩ to the surface resistance because of the shorter beam tubes.

In Fig. 5 SC-IB and RDT2 recent test results after Nb₃Sn coating at 2 K are plotted together with the characteristic test result from the cavity coated in the old coating chamber,

Nb₃Sn COATING OF CEBAF 5-CELL CAVITIES

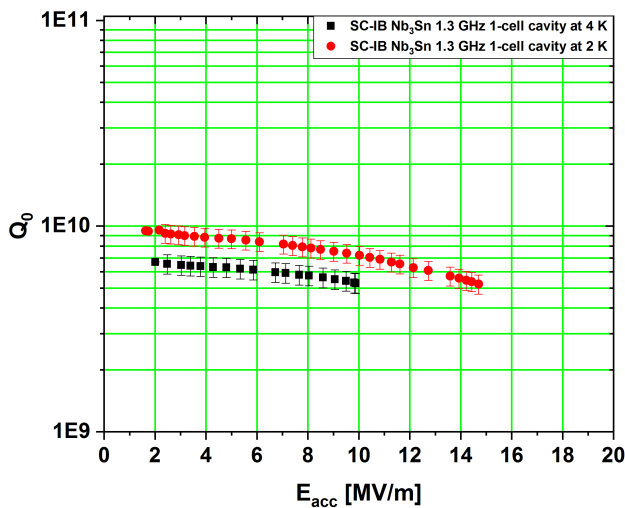


Figure 4: SC-IB test results at 4K and 2K. Low-field quality factors is lower than typical, but note the absence of a rapid Q-drop.

quality factors measured on Wuppertal-coated cavity, and measured on the cavity coated at Cornell. Notably, SC-IB does not exhibit "Wuppertal" Q-slope up to the highest field. As discussed earlier this can be attributed to the absence of titanium in the new coating chamber. However, RDT2, which was coated together with SC-IB, shows a Q-slope at a lower field. It is hard to estimate how much the cold leak and X-rays contributed to the quality factor degradation of RDT2. Further work to re-process as well as re-coat these cavities is in progress to elucidate the cause of Q-degradation.

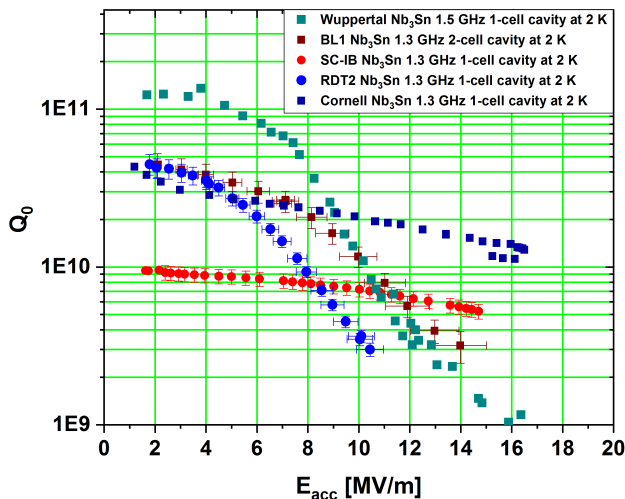


Figure 5: SC-IB and RDT2 recent Q-curves at 2 K are plotted together with a characteristic Q-curve from the cavity coated in the old coating chamber, Q-curve measured on Wuppertal-coated cavity, and Q-curve measured on the cavity coated at Cornell. Notably, SC-IB does not exhibit "Wuppertal" Q-slope up to the highest field.

Following the furnace upgrade, efforts started to coat a complete CEBAF 5-cell cavity. IA320 was used to commission and test the coating procedures for CEBAF cavities. In preparation for Nb₃Sn coating the cavity was high pressure water rinsed and dried in the cleanroom for a couple days. After drying, the cavity was assembled in the cleanroom. During assembly, cavity ports were covered with niobium blanks, which were bolted to the flanges using molybdenum hardware. The bottom beam tube of the cavity was covered with a crucible containing 3 g of SnCl₂ and 10 g of Sn. After the assembly the cavity was moved into the room, where the coating system is located. The cavity was loaded onto the specially made niobium support plate and loaded into the coating system. For Nb₃Sn coating we applied the same heating profile as with the previous cavities [13]. After the process was completed, the cavity was removed, disassembled, and inspected. The equator regions were also inspected with KEK camera [26]. The first coatings were visually non-uniform. While the bottom of the cavity, where the tin source was located, was commonly found to have a complete uniform Nb₃Sn coating, the top two cells of the cavity were consistently found visually distinct suggesting non-uniform coating. After several IA320 coatings it was discovered that one source of the non-uniformity could have been the damage to the top hot-zone element of the furnace and the top thermocouple. After the damaged elements were replaced, IA320 was coated again, but the coating appearance was still not uniform. It was also observed that only several grams out of 10 g of tin were evaporated during the coating. To increase the amount of evaporated tin, and, hence, improve tin coverage of the surface, the heating times were extended, and the nominal anneal temperature was increased to 1250 °C. The modified process resulted in a more uniform coating, although the difference between the top and the bottom was still visible. Despite the difference IA320 was progressed to RF test. The cavity demonstrated a high quality factor at low fields. Quality factor was measured close to 2·10¹⁰ at 4 K and close to 1·10¹¹ at 2 K at low fields. However, the cavity was limited by a strong Q-slope. The maximum accelerating gradients were 2 MV/m at 4 K and 3 MV/m at 2 K limited by quench. The cavity was also tested in π/5-mode of TM₀₁₀. Both higher quality factors and higher gradients were measured in this mode, which suggested that the cavity limitations in π-mode was likely due to coating non-uniformity in the end cell.

The same process was then applied to two more CEBAF cavities, IA110 and IA114. Both coatings were found to have up-down asymmetry again. Similar coating appearance was observed on one of the niobium blanks covering the field probe port on the cavity. The cover was then inspected in SEM/EDS, which revealed that despite its visual appearance the surface was coated with Nb₃Sn, but had a lot of thin Nb₃Sn regions, which sometimes referred to as "maria" in analogy to lunar maria. EDS spectra indicated

Content from this work may be used under the terms of the CC BY 3.0 licence (© 2018). Any distribution of this work must maintain attribution to the author(s), title of the work, publisher, and DOI.

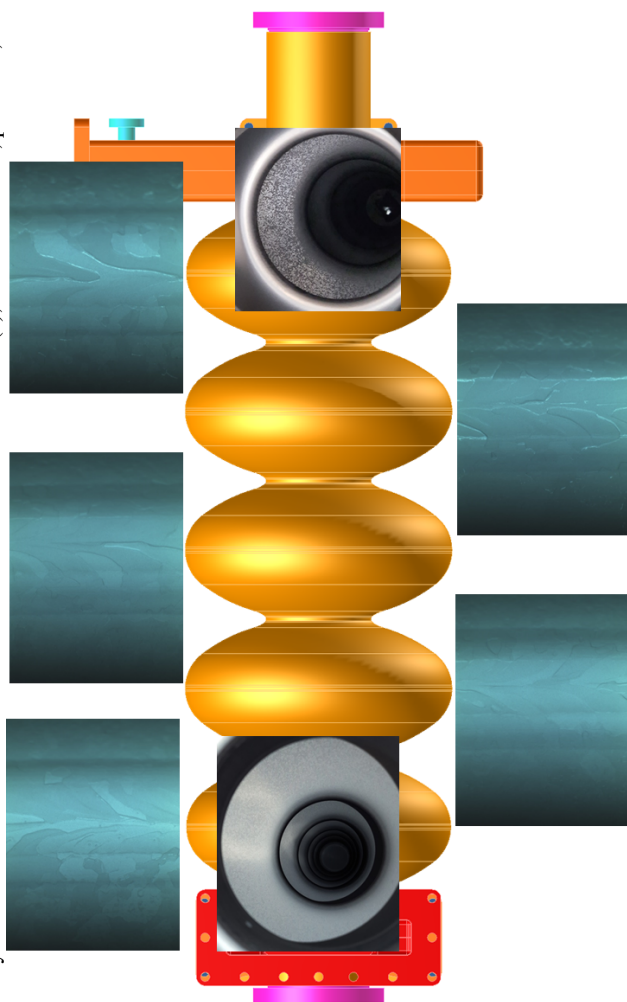


Figure 6: The second coating of IA320. The left column shows equator regions imaged with KEK camera for the first [bottom], third [center], and fifth [top] cells. The right column shows equator regions for the second [bottom] and fourth [top] cells as counted from FPC side. The tin source is attached to the bottom flange of the cavity. The cavity is supported by the top flange as shown in Fig. 1.

that the regions with the regular Nb₃Sn grain structure had about 25 at. %, while maria had about 20-22 at. % of tin. This finding encouraged us to measure the quality factors of these cavities, so both cavities were progressed towards cold RF tests. The low-field quality factor in both cavities was in the mid-10⁹ range at 4 K, which improved to upper-10⁹ range at 2 K. The cavity quench field was about 4-5 MV/m. These cavities are candidate cavity to be used for the quarter cryomodule, but the quality factors and the quench fields need to be improved. The work is in progress to re-process these cavities.

SUMMARY AND FUTURE PLANS

Nb₃Sn deposition system has been upgraded to coat CEBAF 5-cell cavities with Nb₃Sn using vapor diffusion-based

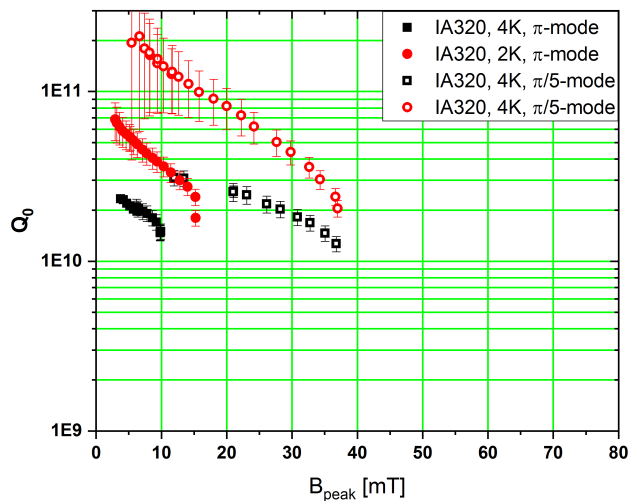


Figure 7: IA320 test results in π - and $\pi/5$ -modes. Higher quality factor and higher quench field suggest that π -mode was likely limited by the end cell.

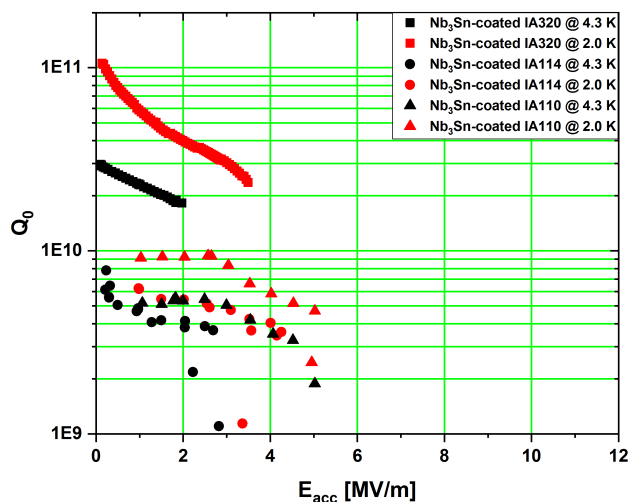


Figure 8: IA320, IA110, and IA114 test results.

process. Several 1-cell and CEBAF 5-cell cavities were coated and tested.

Single-cell measurements indicated possibility of reaching $E_{acc} \cong 15$ MV/m without "Wuppertal" Q-slope in the upgraded system. Further tests are in progress to elucidate the cause behind the Q-slope.

CEBAF 5-cell cavity coatings were found to be non-uniform. Despite non-uniformity, the quality factors above $3 \cdot 10^{10}$ at 4 K and in excess of 10^{11} at 2 K were measured. The accelerating gradients were limited to 2-5 MV/m. Further work is in progress to improve the coating non-uniformity and to achieve accelerating gradients useful for cryomodule use.

ACKNOWLEDGMENTS

We thank JLab technical staff for help with some of the cavity preparation and Larry Phillips, Tony Reilly, Bob Rimmer, Anne-Marie Valente-Feliciano for useful suggestions.

REFERENCES

- [1] D.L. Hall, M. Liepe, R.D. Porter, T. Arias, P. Cueva, D. Liarte, D.A. Muller, J.P. Sethna, N. Sitaraman, in Proc. 18th Int. Conf. on RF Superconductivity, pp. 667-673, Lanzhou, China, (2017).
- [2] G.J. Rosaz, S. Aull, E.A. Ilyina, A. Sublet, and W. Venturini Delsolaro, presented at the 18th Int. Conf. on RF Superconductivity, unpublished, Lanzhou, China, (2017).
- [3] S. Posen, M. Merio, A. Romanenko, and Y. Trenikhina, in Proc. 17th International Conference on RF Superconductivity, pp. 678-680, Whistler, BC, Canada, (2015).
- [4] U. Pudasaini, G.V. Eremeev, M.J. Kelley, C.E. Reece, and J. Tuggle, in Proc. 18th Int. Conf. on RF Superconductivity, pp. 894-899, Lanzhou, China, (2017).
- [5] L. Xiao, X.Y. Lu, W.W. Tan, D. Xie, D.Y. Yang, Y. Yang, Z.Q. Yang, J. Zhao, in Proc. 18th Int. Conf. on RF Superconductivity, pp. 131-133, Lanzhou, China, (2017).
- [6] E. Saur and J. Wurm, Kurze Originalmitteilungen, Die Naturwissenschaften, pp. 127-128 (1962).
- [7] B. Hillenbrand and H. Martens, Jour. Appl. Phys., 47(9):4151-4155 (1976).
- [8] J. Stimmell, PhD dissertation, Cornell University (1978).
- [9] P. Kneisel, O. Stoltz, and J. Halbritter, IEEE Trans. Mag., 15(1):21-24 (1979).
- [10] G. Arnolds, H. Heinrichs, R. Mayer, N. Minatti, H. Piel, and W. Weingarten, IEEE Trans. Nucl. Sci., 26(3):3775-3777 (1979).
- [11] G.V. Eremeev, W.A. Clemens, K. Macha, H. Park, R.S. Williams, in Proc. 16th International Conference on RF Superconductivity, pp. 603-606, Paris, France, (2013).
- [12] G. Müller, P. Kneisel, D. Mansen, H. Piel, J. Pouryamout, and R. W. Roth, in Proc. 6th European Accelerator Conference, 3:2085-2087 (1996).
- [13] G.V. Eremeev, M.J. Kelley, U. Pudasaini, C.E. Reece, and J. Tuggle, in Proc. 17th International Conference on RF Superconductivity, pp. 505-511, Whistler, BC, Canada, 13-18, (2015).
- [14] S. Posen, M. Liepe, Proc. in Proc. 16th International Conference on RF Superconductivity, pp. 666-669, Paris, France, (2013).
- [15] S. Posen, M. Liepe, and D. L. Hall, Appl. Phys. Lett. 106, 082601 (2015).
- [16] S. Posen and D.L. Hall, Supercond. Sci. Technol. 30 033004 (2017).
- [17] J. Tuggle, G.V. Eremeev, M.J. Kelley, C.E. Reece, and H. Xu, in Proc. 17th International Conference on RF Superconductivity, pp. 669-672, Whistler, BC, Canada, 13-18, (2015).
- [18] G.V. Eremeev, M.A. Drury, J.M. Grames, R. Kazimi, M. Poelker, J.P. Preble, R. Suleiman, Y.W. Wang, M. Wright, in Proc. 28th Linear Accelerator Conference, pp. 155-157, East Lansing, MI, U.S.A. (2016).
- [19] G. Arnolds, H. Heinrichs, R. Mayer, N. Minatti, H. Piel, and W. Weingarten, IEEE Transactions on Nuclear Science, 26(3):3775-3777, (1979).
- [20] Ed.: D. Proch, Technical Report TESLA 2000-15, DESY, (2000).
- [21] D.L. Hall, T. Gruber, J.J. Kaufman, M. Liepe, J.T. Maniscalco, S. Posen, Th. Proslie, B. Yu, in Proc. 17th International Conference on RF Superconductivity, pp. 501-504, Whistler, BC, Canada, (2015).
- [22] J. Tuggle et al, to be published.
- [23] P. Dhakal, G. Ciovati, G. R. Myneni, K. E. Gray, N. Groll, P. Maheshwari, D. M. McRae, R. Pike, T. Proslie, F. Stevie, R. P. Walsh, Q. Yang, and J. Zasadzinski, Phys. Rev. ST-AB, 16, 042001 (2013).
- [24] M. Peiniger, PhD dissertation, Wuppertal University (1989).
- [25] J. Knobloch, PhD dissertation, Cornell University (1997).
- [26] Y. Iwashita, Y. Tajima, and H. Hayano, Phys. Rev. ST Accel. Beams 11, 093501 (2008).